Systematic variations in apparent topographic height as measured by noncontact atomic force microscopy

K.-M. Yang, J. Y. Chung, M. F. Hsieh, S.-S. Ferng, and D.-S. Lin*
Institute of Physics, National Chiao-Tung University, 1001 Ta-Hsueh Road, Hsinchu 30010, Taiwan

T.-C. Chiang
Department of Physics, University of Illinois, 1110 W. Green Street, Urbana, Illinois 61801-3080, USA and Frederick Seitz Materials Research Laboratory, University of Illinois, 104 S. Goodwin Avenue, Urbana, Illinois 61801-2902, USA

(Received 30 October 2006; published 21 November 2006)

A flat Si(100) surface is prepared with neighboring n- and p-doped regions. The contact potential difference between the tip and the two well-defined regions of similar material is utilized to examine the effects and interplay of essential tip-sample forces in atomic force microscopy. Measurements with a frequency-modulated noncontact atomic force microscope (NCAFM) show large apparent topographic height variations across the differently doped regions. The height differences depend on the bias polarity, bias voltage, radius, and conducting state of the tip. The functional relationships are well explained by integrated model calculations. These findings provide a coherence scenario of NCAFM operation under these essential forces and facilitate quantitative understanding of the systematic errors in surface topographic height measurement commonly performed in nanoscience.

DOI: 10.1103/PhysRevB.74.193313 PACS number(s): 68.37.Ps, 07.79.Lh, 68.55.−a, 87.64.Dz

Atomic force microscopy (AFM) is a technique widely used for measuring surface morphologies.[1] In most high-resolution applications a noncontact mode is preferred, as it avoids damage or modification to the tip and sample surface caused by physical rubbing or collision.[1–3] Frequency-modulated noncontact operation relies on the detection of tip-sample interactions that are of longer range than the chemical forces.[2,4] A feedback mechanism is typically employed to keep the cantilever resonance frequency at a fixed offset relative to the free resonance frequency. The resulting topographs are maps of constant force gradient over the sample surface. However, these may, or may not, represent the true surface morphology. Specifically, a surface with different work functions in different regions can give rise to significant variations in electrostatic force that may affect the height measurements.[5–8] This issue has been widely recognized, and a number of models have been proposed to account for the relationship between the apparent heights and experimental parameters.[7,9,10] Here, we report a detailed analysis of a particularly simple system, Si(100) surfaces that are topographically flat but with alternately p- and n-doped regions. The different dopings give rise to contact potential differences. AFM measurements of these flat surfaces show large apparent topographic height variations up to a few nanometers that depend on the radius, bias polarity, bias voltage, and conducting state of the tip. While the dependence on bias and conducting state is expected because of the electrostatic interaction, the detailed dependence on tip radius is not necessarily obvious. Our observations are well explained by numerical modeling accounting for all essential interactions and geometrical effects. The results illustrate the interplay of different forces that must be considered for a full understanding of the AFM results.

In our experiment, scanning tunneling microscopy (STM) and noncontact AFM measurements were performed in an ultrahigh-vacuum chamber. Commercial heavily doped monolithic Si cantilevers with initial tip radius ~7 nm were used. The force constant k of the cantilever was ~42 N/m and the free resonance frequency f_0 was ~260 kHz. Metallic tips were also used in the experiment; these were prepared by coating the same Si tips with layers of Cr and $PtIr_5$. Images were taken with a cantilever oscillation amplitude of ~16 nm and a frequency offset $\Delta f = -30$ Hz. The samples used were lightly n-doped Si(100) wafers with a phosphorus doping concentration of 3×10^{14} cm^{-3}. Standard ion-implantation and photolithographic techniques for semiconductor manufacturing were employed to create patterns of heavily p-doped regions with boron as the implanted impurity at a concentration level of 10^{18} cm^{-3}. The sample was annealed to remove implantation damage, acid etched, and then terminated with hydrogen just before insertion into the measurement chamber.

Figure 1 presents the main results. Shown are four rows of STM and AFM images, corresponding to four different tips, numbered I–IV. Tips I and II are both metal-coated tips, but tip II has a substantially larger tip radius than tip I due to extensive use. Tip III is a Si tip with a native SiO_2 overlayer. At the end of the experiment involving tip III, the tip was moved to a different location on the sample surface, and the oxide layer was intentionally rubbed off to make tip IV. Each image in Fig. 1, of size 6×6 μm^2, includes a 3×3 μm^2 area near the center, which is clearly visible in most of the images. This is an area masked off during implantation that remains n doped. The surrounding area is p doped by implantation. The images in the first column are STM results obtained from the four tips, except that tip III is nonconducting and cannot be operated in the STM mode. The lack of contrast in the three STM images shows that the surface is topographically flat. The rest of the images in each row, from left to right, are AFM images obtained at tip bias voltages of −5, −1, 0, 1, and 6 V, respectively. The central n-doped region appears topographically lower (higher) than the

 ©2006 The American Physical Society

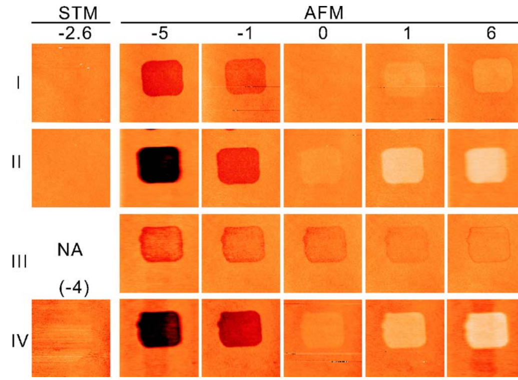

FIG. 1. (Color online) STM (column 1) and AFM images (others) taken with various tip bias V_a in volts for each column as indicated. (The lower left STM image used $V_a = -4$ V.) The images are of size 6×6 μm^2 and have a color (gray) scale for z ranging from −4 to 3 nm. The 3×3 μm^2 area near the center of each image is n doped and surrounded by B-implanted p-doped areas. The frequency shift Δf is −30 Hz.

surrounding areas with a negatively (positively) biased tip, and the height difference depends on the magnitude of the bias voltage. These variations are caused by varying electrostatic forces. Comparing the images in the second row to those in the first row reveals that the contrast variations are substantially larger for a blunt metallic tip. A nonconducting tip (tip III) gives rise to low-contrast variations. The apparent height differences between the n- and p-doped regions, $\Delta z \equiv z_n - z_p$, are deduced from the experiment for various bias voltages and are plotted in Fig. 2 as circles. The substantial differences for the four tips are evident.

To explain the results, we note that the force between a conducting tip structure and the sample,

$$F = F_{apex} + F_{cone} + F_{lever} + F_{vdW}, \quad (1)$$

includes four terms.[2,11–14] The first term is the Coulomb force derived from the apex of the tip, which generally has a conical shape. The second term comes from the tip body, which is approximately in the shape of a truncated cone. The third term comes from the cantilever. Because the Coulomb interaction has a long range, this force is generally not negligible. However, its distance dependence is very weak, corresponding to a negligible force gradient, and therefore its effects can be ignored. The fourth term is the van der Waals force. It is of short range, and is dominated by the tip apex. Chemical forces can be ignored for noncontact operations. Explicit expressions for F_{apex}, F_{cone}, and F_{vdW} can be found in Ref. 14. F_{apex} and F_{cone} depend on the net potential difference V between the tip and the sample, but not F_{vdW}. Physical parameters for the tips used in the experiment are extracted from manufacturing specifications and from our own measurements of the tips.

For a small cantilever oscillation amplitude, the frequency shift due to the tip-sample interaction is proportional to the force gradient.[2,4] The amplitude employed in most experiments, including this one, is actually not sufficiently small for this approximation to hold. A better approximation based on a weighted average is given by

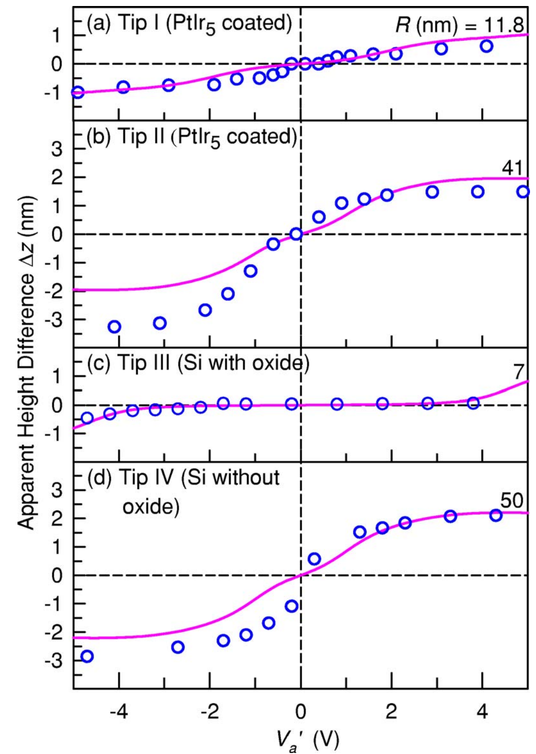

FIG. 2. (Color online) Apparent height differences $\Delta z = z_n - z_p$ (open circles) obtained from the AFM images between the n- and p-doped regions as a function of V_a', where $V_a' = V_a + V_b + (V_c^n + V_c^p)/2$. The solid curves are calculated from Eq. (3). The tip radii used for the calculation are indicated. The calculation for the curve in (c) includes the effect of an oxide layer of 7 nm covering the tip.

$$\Delta f = -\frac{f_0^2}{kA}\int_0^{1/f_0} F[D + A + A\cos(2\pi f_0 t)]\cos(2\pi f_0 t)dt, \quad (2)$$

where D is the minimum distance between the tip and the sample surface, and A is the amplitude of oscillation.[4] Equation (1), with explicit expressions for the different components, and Eq. (2) together can be numerically solved for a fixed Δf to yield $D(R,V)$, namely, the tip-sample distance in terms of the tip radius R and the potential difference V.

Figure 3 shows the calculated $D(R,V)$ as a function of V for a set of values of R. Each curve has a minimum at $V=0$, because the electrostatic interaction is zero. As V increases, the electrostatic force $F_{apex}+F_{cone}$ increases correspondingly, and so does its gradient. This causes the tip to retract, or D to increase, in order to maintain a constant Δf (or a constant force gradient). The response curves are symmetric; that is, $D(R,V)=D(R,-V)$. This is because the electrostatic force is attractive regardless of the sign of V.

Figure 4 shows, in detail, the relative contributions of the apex, cone, and van der Waals terms to Δf in Eq. (2) for two different tip radii. The apex and cone terms vanish at $V=0$. As V increases, the apex term rises rapidly due to an increasing electrostatic force. The tip retracts, and D increases. But this change is counteracted by the van der Waals term, which diminishes rapidly for increasing D, as its a short-range

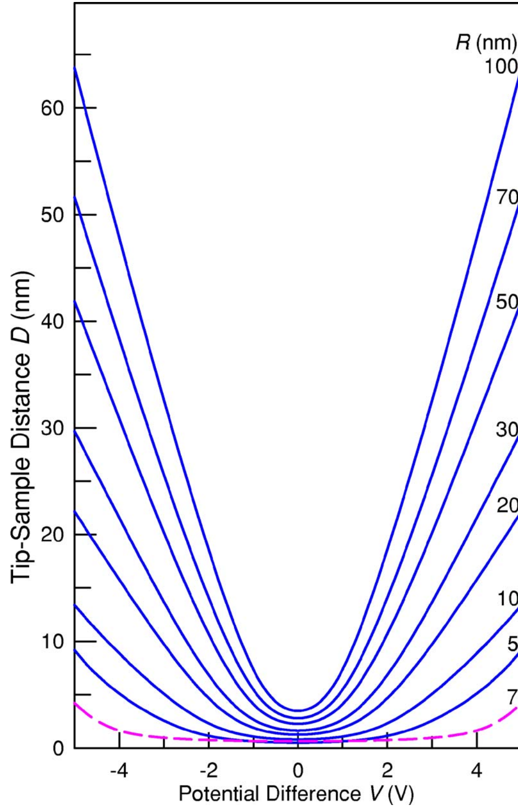

FIG. 3. (Color online) The minimum tip-sample distance D calculated for various tip radii as indicated. The dashed curve is calculated by assuming an oxide layer of 7 nm at the tip's end. Parameters: f_0=260 kHz, Δf=−30 Hz, k=42 N/m, Hamaker constant $H=4\times10^{-19}$ J,[17] θ_{cone}=25°.

interaction. The cone term also rises, but much more slowly, as the distance between the cone and the sample is larger. It becomes important only at large biases. The counteracting effect of the van der Waals term accounts for the relatively flat response near $V=0$ for the curves in Fig. 3. This discussion illustrates that the van der Waals force, while

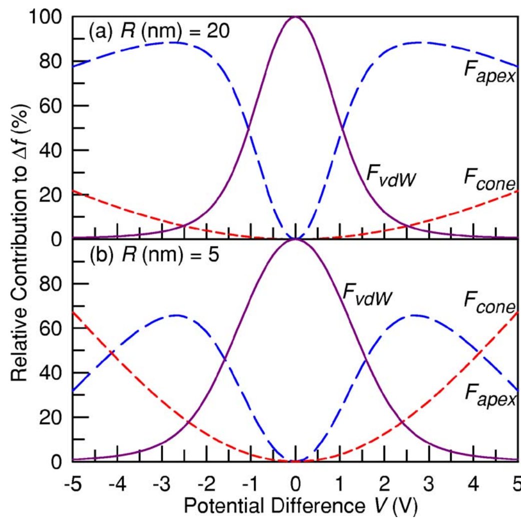

FIG. 4. (Color online) Individual contributions to Δf from the various component forces as indicated.

independent of the potential difference V at a fixed distance, can be an important contribution to the overall response of the system when the tip moves.

For a conducting sample, the net potential difference V between the tip and sample consists of three terms: the contact potential difference V_c, the applied tip bias voltage V_a, and an effective built-in bias V_b for insulating tips caused by stray static charges.[15,16] For a fixed V_a+V_b, $D(R,V)$ depends on V_c. This dependence leads to the apparent topographic height differences between the n- and p-doped regions. Explicitly,

$$\Delta z(R,V_a) \equiv z_n - z_p = D(R,V_a+V_b+V_c^n) - D(R,V_a+V_b+V_c^p), \quad (3)$$

where V_c^n and V_c^p are the tip-sample contact potential differences in the n- and p-doped regions, respectively. These contact potential differences as well as V_b can be determined from a measurement of the resonance frequency shift as a function of V_a. The results show that $V_c^n - V_c^p$=0.2 V, which agrees with an independent Kelvin force microscopy measurement. Similar measurements were reported earlier and the results were attributed to the effects of surface states and adsorbate-induced states.[18,19] If the bias voltage is chosen to compensate for V_b and the average of the two contact potential differences

$$V_a = -V_b - \frac{1}{2}(V_c^p + V_c^n), \quad (4)$$

one finds

$$\Delta z = D\left(R, \frac{V_c^n - V_c^p}{2}\right) - D\left(R, \frac{V_c^p - V_c^n}{2}\right) = 0. \quad (5)$$

Thus, the height difference becomes zero for this particular choice of the applied bias. This is a special case of interest previously investigated in an experimental study.[5]

The quantity Δz as a function of V_a' can be computed from Eq. (3), where $V_a' = V_a + V_b + (V_c^n + V_c^p)/2$. The results are shown as solid curves in Fig. 2. The tip radii used in the calculation are indicated in the figure. These values are deduced from separate measurements of D as a function of V, and are consistent with the manufacturer's specifications and/or our own measurements with an electron microscope. As seen in Fig. 2, the calculated results are in good agreement with the data for positive bias voltages. For negative bias voltages, the results are expected to be just a negative mirror image of the results for positive bias voltages, because Δz is an odd function of V. However, the data for tips II and IV fall significantly below the calculated results. The reason for the discrepancies has to do with the low doping level in the n-doped region of the sample. Tips II and IV have relatively large tip radii. With a negative bias on these large tips, the small number of carriers in the lightly n-doped region of the sample can be partially depleted, leading to a smaller electrostatic interaction than expected based on the model discussed above. This causes a reduction in D for a negative bias, or equivalently, an apparent reduction in the

height of the *n*-doped region. The other two tips, I and III, have much smaller radii, and are not appreciably affected by this effect.

The results taken with tip III show much smaller height variations. Separated by the nonconducting native oxide layer in addition to *D*, the distance between the conducting parts of the tip and the sample is larger than that of a conducting tip with the same tip geometry. The electrostatic interaction is therefore very much reduced while the van der Waals contribution remains about the same. The dashed curve shown in Fig. 3 is obtained by assuming a 7-nm-thick oxide on a conducting body with an apex radius of 7 nm based on the manufacturer's specifications. Within $\sim\pm 3$ V, the tip-sample distance remains fairly constant because F_{apex} and F_{cone} are insignificant at such small biases and the van der Waals term is insensitive to potential changes. This model leads to the calculated curve shown in Fig. 2(c), which agrees well with the data.

The seemingly complex dependencies of the apparent topographical height variations on the radius, bias, and conducting state of the tip, as seen in Fig. 2, are thus well explained. The work function difference between the *n*- and *p*-doped regions on the Si substrate is just 0.2 eV. Yet the resulting apparent height differences can be as large as a few nanometers depending on the details of the tip. This behavior can be related to the steep slopes of the response curves seen in Fig. 3 at large biases where the counteracting effect of the van der Waals contribution diminishes.

In conclusion, we have performed a detailed study of the response of an AFM operating in a frequency-modulated noncontact mode that is widely employed in surface morphology measurements. We further applied the numerical analysis to a well characterized test sample and so the systematics of the data can be understood unambiguously. The aim is to achieve a level of quantitative understanding of the effects and interplay of the various forces between the tip and sample, to generate a coherent picture of noncontact AFM operation under these essential forces, and to provide the user community a useful quantitative estimation for the systematic errors in surface topographic height measurement. With a test sample of Si(100) that is topographically flat but with a surface pattern of alternately doped areas, we have experimentally examined the effects of the work function variations on the apparent topographical height as a function of the radius, bias, and conducting state of the tip. The results show large apparent topographical variations with seemingly complex functional relationships. The results are nevertheless well explained by a full analysis accounting for all essential interactions in the system. Similar results were obtained for the amplitude-modulated AFM due to their similarity in operation principle.[20]

This work is supported by the National Science Council of Taiwan under Contract No. NSC 94-2112-M009-010 (D.S.L.), by Center for Nano Science and Technology, National Chiao-Tung University (D.S.L.), by the U.S. National Science Foundation under Grant No. DMR-05-03323 (T.C.C.), and by the Petroleum Research Fund, administered by the American Chemical Society (T.C.C.).

*Electronic address: dslin@mail.nctu.edu.tw

[1] Ernst Meyer, Hans J. Hug, and Ronald Bennewitz, *Scanning Probe Microscopy: The Lab on a Tip* (Springer, Berlin, 2003).
[2] *Noncontact Atomic Force Microscopy*, edited by S. Morita, R. Wiesendanger, and E. Meyer (Springer, Berlin, 2002).
[3] M. Lee and W. Jhe, Phys. Rev. Lett. **97**, 036104 (2006).
[4] F. J. Giessibl, Rev. Mod. Phys. **75**, 949 (2003), and references therein.
[5] S. Sadewasser and M. Ch. Lux-Steiner, Phys. Rev. Lett. **91**, 266101 (2003).
[6] T. Arai and M. Tomitori, Appl. Surf. Sci. **188**, 292 (2002).
[7] R. Bennewitz, A. S. Foster, L. N. Kantorovich, M. Bammerlin, Ch. Loppacher, S. Schär, M. Guggisberg, E. Meyer, and A. L. Shluger, Phys. Rev. B **62**, 2074 (2000).
[8] S. Morita, M. Abe, K. Yokoyama, and Y. Sugawara, J. Cryst. Growth **210**, 408 (2000).
[9] Y. Rosenwaks, R. Shikler, Th. Glatzel, and S. Sadewasser, Phys. Rev. B **70**, 085320 (2004).
[10] S. Sadewasser, Ph. Carl, Th. Glatzel, and M. Ch. Lux-Steiner, Nanotechnology **15**, S14 (2004).
[11] L. Olsson, N. Lin, V. Yakimov, and R. Erlandsson, J. Appl. Phys. **84**, 4060 (1998).
[12] G. M. Sacha, A. Verdaguer, J. Martínez, J. J. Sáenz, D. F. Ogletree, and M. Salmeron, Appl. Phys. Lett. **86**, 123101 (2005).
[13] M. S. Jean, S. Hudlet, C. Guthmann, and J. Berger, J. Appl. Phys. **86**, 5245 (1999).
[14] J. Colchero, A. Gil, and A. M. Baró, Phys. Rev. B **64**, 245403 (2001).
[15] R. Dianoux, F. Martins, F. Marchi, C. Alandi, F. Comin, and J. Chevrier, Phys. Rev. B **68**, 045403 (2003).
[16] E. M. Muller and J. A. Marohn, Adv. Mater. (Weinheim, Ger.) **17**, 1410 (2005).
[17] M. Guggisberg, M. Bammerlin, Ch. Loppacher, O. Pfeiffer, A. Abdurixit, V. Barwich, R. Bennewitz, A. Baratoff, E. Meyer, and H.-J. Güntherodt, Phys. Rev. B **61**, 11151 (2000).
[18] C. Loppacher, U. Zerweck, S. Teich, E. Beyreuther, T. Otto, S. Grafström, and L. M. Eng, Nanotechnology **16**, S1 (2005).
[19] A. Kikukawa, S. Hosaka, and R. Imura, Appl. Phys. Lett. **66**, 3510 (1995).
[20] Y. T. Wu, M.S. thesis, National Chiao-Tung University, Taiwan, 2006.